IOPscience iopscience.iop.org

Home Search Collections Journals About Contact us My IOPscience

Small self-interstitial clusters in GaAs

This article has been downloaded from IOPscience. Please scroll down to see the full text article.

2003 J. Phys.: Condens. Matter 15 843

(http://iopscience.iop.org/0953-8984/15/6/311)

View the table of contents for this issue, or go to the journal homepage for more

Download details:
IP Address: 171.66.16.119
The article was downloaded on 19/05/2010 at 06:33

Please note that terms and conditions apply.

INSTITUTE OF PHYSICS PUBLISHING JOURNAL OF PHYSICS: CONDENSED MATTER

J. Phys.: Condens. Matter **15** (2003) 843–853 PII: S0953-8984(03)55324-3

Small self-interstitial clusters in GaAs

G Zollo[1] **and R M Nieminen**[2]

[1] Department of Energetics, University of Rome 'La Sapienza' and INFM, via Antonio Scarpa 14-16, 00161 Rome, Italy
[2] COMP/Laboratory of Physics, Helsinki University of Technology, PO Box 1100, 02015 HUT, Finland

Received 25 October 2002
Published 3 February 2003
Online at stacks.iop.org/JPhysCM/15/843

Abstract
Recent studies have shown evidence for the aggregation of self-interstitials in ion-implanted Si, resulting in nanoscopic damage structures. Similarly, self-interstitial atoms are expected to play an important role for defect clustering in ion-implanted GaAs. Accurate first-principles total-energy calculations are reported for different As and Ga self-interstitial configurations. These results are used to study by first-principles total-energy calculations the structural and electronic properties of small complexes involving self-interstitials and/or antisites.

(Some figures in this article are in colour only in the electronic version)

1. Introduction

There has been long-standing interest in III–V compound semiconductors, in particular GaAs as the prototype of the III–V family. Many aspects related to native defects and defects introduced by electron and ion irradiation have been clarified during the past decade [1–3]. However, while a number of defect-associated deep levels have been observed and assigned to various defect families (such as EL2), their atomistic structures remain at least partially unresolved. In the case of GaAs, the energies of different electronic levels designated as EL2 in fact vary from one sample to another, depending on the implantation conditions. Thus these defects must be associated with different atomistic structures [4–9].

In general, both the measured and calculated formation energies of point defects favour the presence of vacancies and antisites over self-interstitials in as-grown material in thermodynamic equilibrium [10]. However, implanted materials can be far from thermodynamic equilibrium, and thus the presence of self-interstitials must be taken into account in addition to vacancies and antisites. As interstitials can be highly mobile, one expects that they can easily form bigger aggregates. A similar situation prevails in Si where the extended ⟨311⟩ defects are formed via self-interstitial aggregation. At the moment, no experimental technique is able to directly detect simple self-interstitials in III–V semiconductors, but

 © 2003 IOP Publishing Ltd Printed in the UK

experimental observations have shown that nanoscale aggregates do form in implanted material [11–14]. In particular, in the case of GaAs, high-resolution transmission electron microscopy (HRTEM) observations give some indications on the inner topology of such aggregates, but do not resolve their atomic structure [15]. Reliable models of nanoscale aggregates in GaAs have been developed only for vacancy clusters [16].

The electronic characterization of defect aggregates in implanted III–V compound semiconductors is thus an open problem, the solution of which should take advantage of reliable atomistic models and their calculated electronic properties. In this paper we first address the problem of accurate modelling of single Ga and As self-interstitials. The modelling of these defects has earlier been addressed by other authors [10, 17]. Using enhanced computational resources, we argue here that some of the earlier conclusions should be revised. We then focus our attention to As self-interstitials and their complexes in order to clarify some of their basic properties. The reason for addressing mainly As clustering is that defects such as As antisites, As interstitials and their complexes seem to be responsible for the semi-insulating electrical properties of as-implanted GaAs [4, 18], similarly to what has been earlier observed for low-temperature (LT) grown GaAs [19, 20].

2. Methods

We use the density-functional theory (DFT) [21] and the local-density approximation (LDA) [22]. The calculations are performed using the self-consistent total-energy pseudopotential (PP) method. The Perdew–Zunger [23] parametrization of the Ceperley–Alder data [24] is used for the exchange–correlation energy. Norm-conserving Hamann PPs [25] in the Kleinman–Bylander form [27] have been used for both Ga and As atoms. The valence-electron wavefunctions are expanded in a plane-wave basis set up to a kinetic energy cut-off of 28 Ryd. We mainly use the $2 \times 2 \times 2$ Monkhorst–Pack (MP) [26] k-point Brillouin zone sampling and 64-atom supercells (SCs). We use the LDA approximation also for unpaired spins because the energy differences with respect to spin-polarized calculations (LSDA) are expected to be small.

The total-energy calculations and consequently the optimal geometries can be affected by spurious defect–defect elastic interactions and the dispersion of the electronic gap states due to the SC approach. It has been shown [28] that for a single vacancy in Si the calculation in a 216-atom SC with the Γ point sampling has converged both for the geometry and the energy, the latter quantity being less sensitive to the computational parameters. In order to evaluate the convergence of our calculations, we have also performed several test calculations using 216-atom SCs, the Γ point sampling and different cut-off energies.

3. Results and discussions

According to our calculations, the equilibrium lattice constant in the zincblende structure and the heat of formation ΔH for GaAs are 5.55 Å and 1.0 eV, respectively. The experimental values are 5.65 Å and 0.75 eV. The calculated bandgap at the Γ point is 1.08 eV while the experimental value is 1.517 at 0 K. The obtained values are close to previous DFT calculations, which (like ours) are affected by the well known problems of overbinding and gap underestimation inherent in the LDA approximation. We also calculate the neutral As antisite as a reference to be compared to other calculations. The obtained formation energy is 2.48 eV, close to the previous values of 2.5 [29] and 2.29 eV [31]. However, both of the earlier reported values have been obtained with a smaller SC and less accurate k-point sampling schemes. According to our calculations, the As antisite is stable in the neutral and +2 charge states, and the thermodynamic transition (ionization level) between these states is 89 meV above the valence band maximum (VBM).

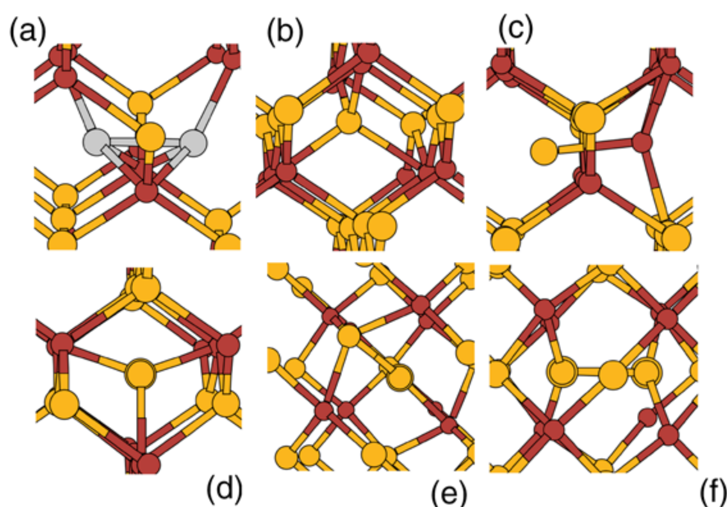

Figure 1. Main interstitial configurations: (a) the ⟨110⟩ dumbbell; (b) the tetrahedral site; (c) the ⟨110⟩ dumbbell at the hetero site; (d) the hexagonal site; (e) the twofold site—the interstitial is between two bonded atoms along the ⟨110⟩ direction; (f) the ⟨100⟩ dumbbell.

Table 1. Formation energy E_f of the neutral As interstitial for various geometries (see figure 1).

	⟨110⟩ dumbbell	⟨110⟩ dumbbell (Ga site)	Tetrahedral	Hexagonal	Twofold	⟨100⟩ dumbbell
E_f (eV)	4.07	4.64	5.04	Unstable: relaxes to tetrahedral	Unstable: relaxes to ⟨110⟩ dumbbell	Unstable: relaxes to ⟨110⟩ dumbbell

Table 2. Formation energy E_f for the neutral Ga interstitial for various geometries (see figure 1).

	⟨110⟩ dumbbell	⟨110⟩ dumbbell (As site)	Tetrahedral	Hexagonal	Twofold	⟨100⟩ dumbbell
E_f (eV)	3.53	3.99	2.98	Unstable: converges to tetrahedral	Unstable: converges to tetrahedral	Unstable: converges to tetrahedral

3.1. Single self-interstitials

We investigate possible structures for both the As and Ga self-interstitials, namely the ⟨110⟩ and ⟨100⟩ dumbbells, the tetrahedral and hexagonal sites and the twofold geometry, as depicted in figure 1. The formation energies E_f for the neutral defects are reported in tables 1 and 2.

The stable configurations for both the neutral Ga and As self-interstitials are the ⟨110⟩ dumbbell (both atomic sites) and the tetrahedral site. For As the homo-atomic ⟨110⟩ dumbbell has the lowest formation energy. The hexagonal, the twofold and the ⟨100⟩ dumbbell configurations, which have been previously proposed, are unstable. The general trend is that the formation energies for Ga interstitials are lower than for the As interstitials. In particular,

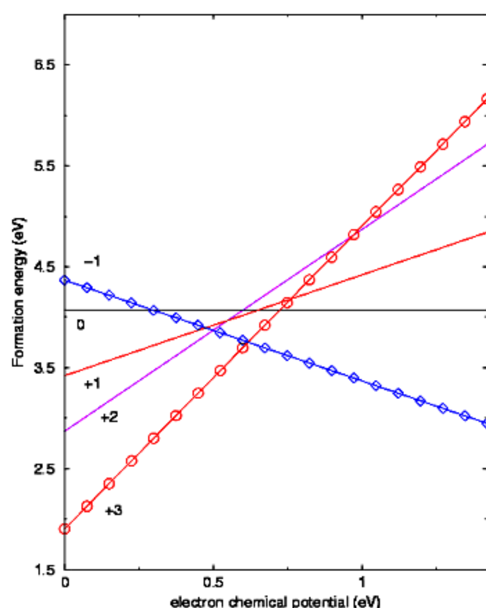

Figure 2. The formation energies of the As⟨110⟩ dumbbell in various charge states (see the labels) as functions of electron chemical potential in stoichiometric GaAs. The stable charge states are +3 and −1.

the Ga tetrahedral has a low energy not far from the As antisite, which is known to be present in as-grown GaAs. Therefore the Ga self-interstitial concentration could be considerable even in as-grown GaAs. In contrast, the formation energy of the most stable As self-interstitial (the ⟨110⟩ dumbbell) is about 1 eV higher (although much lower than the values previously reported in the literature [29]). Thus an observable concentration of such defects seems unlikely in as-grown GaAs. However, in ion-implanted GaAs, single As and Ga interstitials should be formed independently of their formation energies, being produced by the collision events in the matrix.

3.2. The As⟨110⟩ dumbbell

We now focus our attention on the most stable As self-interstitial configuration, the ⟨110⟩ As dumbbell, for which we also investigate the various charge states. In figure 2 we report the formation energies of charged defects for stoichiometric GaAs, drawn as functions of the electronic chemical potential, calculated using the formulation of Zhang and Northrup [10]. For the electrostatic interactions between the charged defects and their replicas we applied basically the Makov–Payne [30] formula for the Ewald correction. As is clearly shown, the thermodynamically stable charge states are +3 and −1, and the ionization level (+3| − 1) is located about 0.62 eV above the VBM, the neutral charge state being metastable. According to our calculations, the As⟨110⟩ dumbbell should thus behave as a strong negative-U system, but differently to what was previously reported by Chadi [17]. Chadi used a small (32-atom) SC and a low cut-off energy.

The As⟨110⟩ dumbbell thus behaves as a deep acceptor with a well defined fingerprint, the transition level at 0.62 eV from the VBM. If present, it should be detectable by spectroscopic (e.g. DLTS) techniques. The symmetry properties of the structures of the As⟨110⟩ dumbbell at different charge states are reported in table 3. In table 3 and in the following tables reporting

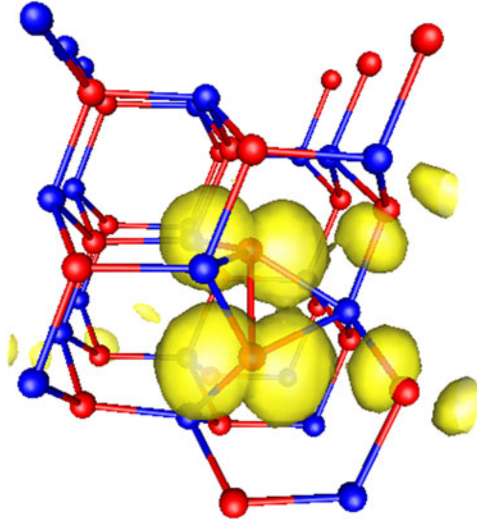

Figure 3. Neutral As⟨110⟩ dumbbell: electron density map obtained from the uppermost Kohn–Sham defect-localized state at 200 meV above the VBM. The displayed state contains one electron.

Table 3. The point symmetry group of the charged As⟨110⟩ dumbbell.

Charge state	−1	0	+1	+2	+3
Symmetry group	C_2	$\sim C_{1h}$	$\sim C_{2v}$	None	C_{1h}

data on the symmetries, we have adopted the following criterion to evaluate how close to the perfect symmetry group one is. We have compared pairs of atomic distances and angles that should be strictly equal in a perfectly symmetric structure. If the highest relative difference is lower than 0.001%, the structure is assigned to the ideal symmetry group; otherwise, the maximum relative difference is reported.

The calculations performed for a 65-atom SC (cut-off 28 Ryd, 2 × 2 × 2 MP sampling) indicate that the neutral defect deviates from the C_{1h} symmetry by about 0.03%, while the singly negative charge state has the C_2 symmetry and the singly positive charge state the C_{2v} symmetry. The neutral As⟨110⟩ dumbbell induces an open volume in the GaAs lattice: the volume of the tetrahedron formed by the four Ga atoms bonded to the As dumbbell atoms is 9.023 versus the 7.12 Å^3 which is the tetrahedron volume in the perfect lattice. The lattice dilation induced by the presence of a ⟨110⟩ dumbbell is therefore around 28% per excess As atom.

The electronic structure has one Kohn–Sham single-electron level in the gap, 200 meV above the VBM, indicating that the As⟨110⟩ dumbbell should behave as a deep acceptor. The two other Kohn–Sham levels are very close in energy and practically located at the VBM at the Γ point. The Kohn–Sham eigenvalues are, of course, affected by the well known problems of LDA–DFT, which include the underestimation of the bandgap in semiconductors and insulators. The Kohn–Sham wavefunction corresponding to the deep acceptor localized level (i.e. corresponding to the eigenvalue about 200 meV above the VBM) contains one electron (if the dumbbell is in the neutral charge state) and has a p character, bonding the As atoms of the dumbbell to the closest Ga atoms as reported in figure 3.

We have also tested the convergence of the calculations for the neutral As⟨110⟩ dumbbell, with particular regard to the elastic interactions between the defect images and the spurious dispersion of the localized defect gap states. The convergence tests are reported in table 4.

Table 4. Convergence tests for the neutral As⟨110⟩ dumbbell.

	65 atoms Γ point 28 Ryd cut-off	65 atoms $2 \times 2 \times 2$ MP 28 Ryd cut-off	65 atoms $2 \times 2 \times 2$ MP 22 Ryd cut-off	217 atoms Γ point 15 Ryd cut-off
E_f (eV)	2.9	4.07	4.09	4.06

A calculation was performed with a 65-atom SC and Γ point sampling in order to check the importance of the Brillouin zone sampling. In order to check the convergence in terms of the cut-off energy, the standard calculation has been repeated using 22 Ryd. Finally, a calculation has been performed with a 217-atom SC by sampling the Brillouin zone with the Γ point and the cut-off energy of 15 Ryd.

We notice that an inaccurate sampling scheme for the 65-atom SC strongly affects the calculation, resulting in a serious underestimation of the formation energy. The $2 \times 2 \times 2$ MP sampling scheme and the larger cut-off energy ensure the convergence of the result in the 65-atom SC, as can be recognized by comparing these results to the one obtained for a 217-atom SC. In such a large SC, the sampling can be reduced to the Γ point only. We can therefore conclude that the formation energy is well converged in a standard calculation ($2 \times 2 \times 2$ MP, 65-atom SC, 28 Ryd cut-off). As mentioned above, the spurious defect-level dispersion and the elastic interactions between the defect images affect the defect structure more than the formation energy. Therefore we have also checked the convergence of the symmetry properties. The optimal geometries of the standard calculations are preserved in the 217-atom SC even though the deviation from the C_{1h} symmetry seems somewhat more pronounced (the bond length differences increase to 0.066%). One can thus be confident that both the formation energy (4.07 eV) and the symmetry properties are well reproduced in a 65-atom SC and the $2 \times 2 \times 2$ MP Brillouin zone sampling.

The stable charge states are +3 and −1, whose symmetry groups are C_{1h} and C_2, respectively. In the first case the mirror plane is the one that contains the two As atoms of the dumbbell and is perpendicular to the ⟨110⟩ direction; in the second case the twofold axis lies along the ⟨100⟩ direction and is perpendicular to the ⟨110⟩ axis of the dumbbell.

3.3. Small As clusters

We have investigated basically two kinds of small cluster involving As self-interstitials and/or As antisites: the As–As self-interstitial cluster (see figure 4) and the As split antisite structure (composed of an As antisite and an As⟨110⟩ dumbbell sharing the same Ga site), see figure 5.

3.3.1. As di-interstitial. The structure of the As–As dumbbell cluster is reported in figure 4. The formation and the binding energies are reported in table 5.

In the 66-atom SC, the binding energy is overestimated by about 140 meV with respect to the value obtained in the 218-atom SC. As concerns the structural properties, the symmetry of the 66-atom SC is quite close to C_{1h} (the differences in the bond lengths vary between 0.004 and 0.14%), where the mirror plane contains the extra As atom added to the pre-existing dumbbell. This feature is also preserved in the case of the 218-atom SC with the bond lengths close to the C_{1h} symmetry (within 0.03–0.4%). The open volume induced in the matrix can be evaluated by measuring the volume of the tetrahedron defined by the four Ga atoms bonded to the As site occupied by the three As atoms. This volume is 9.9 Å^3, i.e. 39% more than the normal volume. Because this structure arranges two extra As atoms in the GaAs lattice,

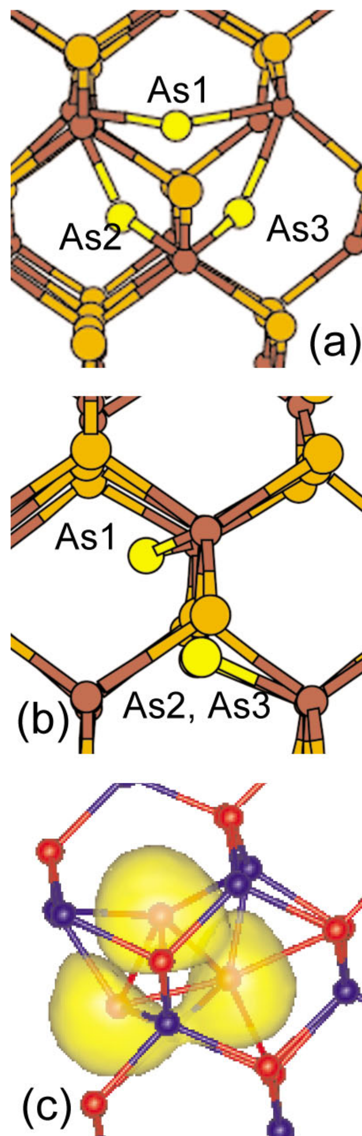

Figure 4. The As⟨110⟩ di-interstitial configuration viewed along two perpendicular ⟨110⟩ directions (a) and (b). The electron isodensity map, obtained by subtracting the bulk isodensity from the isodensity obtained for the di-interstitial, indicates that the extra ten electrons introduced for the neutral As⟨110⟩ di-interstitial are mainly localized at the three As atoms sharing one As site (c).

the lattice dilation per excess As atom is about 20%, clearly less than the lattice dilation per single interstitial but still considerably more than the lattice dilation per excess As induced by a simple As antisite.

The Kohn–Sham eigenvalues related to the defect are located near the maximum of the valence band. The corresponding wavefunctions are not fully localized around the As interstitial complex, although much of their electron density is located close to the three As atoms sharing the As lattice site.

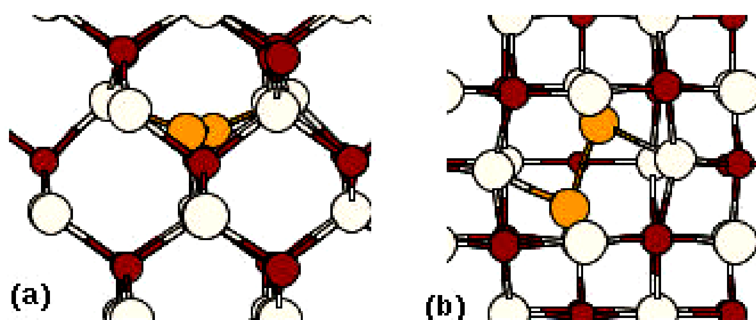

Figure 5. The As split-antisite configuration viewed along the ⟨110⟩ (a) and the ⟨001⟩ (b) directions.

Table 5. (a) Formation and binding energy of the As interstitial cluster. (b) Calculated energies for the As antisite–interstitial complex.

(a)	66 atoms 2 × 2 × 2 MP 28 Ryd cut-off	218 atoms Γ point (not relaxed) 15 Ryd cut-off	218 atoms Γ point relaxed 15 Ryd cut-off
E_f (eV)	5.93	6.18	5.77
$E_b = 2E_{\mathrm{As}\langle 110\rangle} - E_f$	2.21	2.56	2.35
(b)	65 atoms 2 × 2 × 2 MP 28 Ryd cut-off	217 Γ point 15 Ryd cut-off	
E_f (eV)	4.87	5.22	
$E_b = E_{\mathrm{As}\langle 110\rangle} + E_{\mathrm{AsGa}} - E_f$	1.68	1.32	

We can compare the structural and electronic properties obtained in this case to the di-interstitial in Si studied by Kim *et al* [32]. They report a structure quite similar to the present case. The possible transitions between equivalent C_{1h} symmetry structures found in Si are also present in GaAs, and each equivalent C_{1h} symmetry structure can be obtained by a single As migration along one of the ⟨110⟩ directions. The migration arguments have been used by Kim *et al* in order to interpret the $P6$ defect centre, experimentally observed in Si at 300 K and showing a D_{2d} symmetry, in terms of the di-interstitial structure. The transition energy between equivalent C_{1h} configurations was calculated by Kim *et al* to be 0.5 eV. At 300 K, due to such a small barrier, the structure continuously oscillates between the four equivalent C_{1h} states, thus assuming an effectively D_{2d} symmetric character. At low temperatures the thermal energy is not sufficient to let the interstitial overcome the energy barrier and the C_{1h} symmetry is conserved.

In the present case, the As di-interstitial does not have Kohn–Sham levels in the gap. Although the Kohn–Sham states are not the true electron quasiparticle levels, the fact that there are no states in the gap is a strong indication that such a complex cannot be observed by deep-level spectroscopy (e.g. DLTS, PICTS) or by EPR. On the other hand, as already mentioned, As di-interstitials should easily be formed due to their large binding energy and to the commonly presumed high diffusion rates of As interstitials. The lack of experimental results for single As interstitials in as-grown or annealed GaAs could, therefore, be explained in these terms.

3.3.2. As antisite–interstitial complex. In implanted GaAs, as well as in LT grown GaAs, a large concentration of As antisites is expected. Therefore the As interstitial–As antisite complex can be formed if both of the components are provided. This As antisite–As interstitial complex, also called the split antisite, has been earlier proposed to explain the presence of a donor band 0.3–0.5 eV below the conduction band minimum in LT grown GaAs [33]. Moreover, the properties of this complex agree well with EPR and lattice dilation data showing that this complex can contribute only a small amount to the net lattice dilation, the main contribution being accounted for by As antisites observed by EPR. Subsequently, other results for LT GaAs have shown that the presence of such a complex seems to be unlikely, and the lattice dilation and ion channelling data for samples with As excess lower than 1.5% can be well explained by taking into account isolated As antisites only. Earlier theoretical studies for the As antisite may not provide quantitatively reliable data for the formation and binding energies due to the Γ point sampling and SC size [33]. Thus it is also worthwhile to study this defect more carefully and to check whether the computational parameters affect the results.

The atomic structure, reported in figure 4, is very similar to the one obtained by Landmann *et al* [33]: the two As atoms sharing the Ga lattice site are aligned along the $\langle 2\,0\,\bar{1}\rangle$ direction. In the standard calculation the actual geometry deviates slightly from the C_2 symmetry (bond length deviations are around 0.2%). This structure has also been tested in a 217-atom SC (15 Ryd and Γ point sampling), with the main features of the structure confirmed: the two As atoms sharing the Ga lattice site are 2.338 Å apart and are aligned along the $\langle 2\,0\,\bar{1}\rangle$ direction. The deviation from the C_2 symmetry is less pronounced than in the 65-atom SC (bond length deviations less than 0.02%).

In table 5 we report the formation and the binding energies obtained for both the 65- and 217-atom SCs. It appears that by using the 65-atom SC the formation energy is underestimated by about 350 meV and the binding energy overestimated by about the same amount. The binding energy we obtain with respect to the neutral As antisite and As⟨110⟩ dumbbell is about 1.3 eV (obtained with the 217-atom SC). This value, obtained for stoichiometric GaAs, should also be considered valid for LT grown GaAs, characterized by 1.5% As excess [33–35], because the correction due to the unbalanced stoichiometry is small. This value is also close to the formation energy obtained by Landmann *et al* [33] for neutral As antisites and As interstitials (about 1.4 eV) in a 65-atom SC. However, these authors did not calculate the absolute value of the As⟨110⟩ formation energy but used one obtained indirectly, based on the unrelaxed As tetrahedral interstitial that was previously considered by Zhang and Northrup [10].

The open volume induced by the As antisite is measured by evaluating the volume of the tetrahedron formed by the As atoms bonded to the Ga atom whose site is occupied by the As antisite. This volume is about 10.2 $Å^3$ in the 65-atom SC and 10.4 $Å^3$ in the 217-atom SC (43 and 46% larger than the perfect volume, respectively). The lattice dilation induced by such a defect is, therefore, around 15% per excess As atom. This value is lower than reported by Landmann *et al* [33]. Moreover, the value is lower than the lattice dilation per excess As atom obtained for the di-interstitial structure.

The As antisite–interstitial complex seems an efficient way to store excess As atoms, resulting in low lattice dilation per excess As. It is not as efficient as isolated As antisites (10% lattice volume dilation per excess As) but comparable. The electronic structure of the neutral As antisite shows the presence of a Kohn–Sham state, occupied by one electron, at 210 meV below the conduction band minimum. The other defect states are resonant with the valence states. In their paper Landmann *et al* [33] found that the As antisite was characterized by a Kohn–Sham state about 300 meV below the conduction band, which led them to the hypothesis that this complex could be responsible for the donor band found 0.5–0.3 eV below the conduction band. However, such a donor band has not been observed in implanted GaAs

where one would expect to find it if really related to the split antisite. On the basis of our results, obtained by more accurate calculations, this hypothesis seems to be unlikely: the Kohn–Sham level of the As antisite is actually about 200 meV below the conduction band, i.e. outside the experimentally detected donor band. We stress that the use of large SCs is necessary to obtain reliable results. The difference between the Kohn–Sham donor level obtained here and the one reported by Landmann *et al* [33] (210 and 300 meV below the conduction band respectively) excludes the location of this level in the experimentally detected donor band. The authors of [33] also discussed the possible continuous forming and decomposing of such a complex in order to justify the presence of the donor band instead of the simple donor level related to the split antisite. If this were the case, however, one should either observe the split interstitial as well or there should exist some 'interstitial reservoir' with a low binding energy and not easily observable. We have demonstrated, on the contrary, that if an 'interstitial reservoir' exists (such as the di-interstitial), it has a large binding energy which makes its decomposition unlikely.

4. Conclusions

The presence of self-interstitials in GaAs is still controversial in bulk GaAs, even though there is increasing experimental evidence pointing towards their indirect effects. In the case of As self-interstitials the question is particularly intricate, and arguments and experimental results both in favour and against their presence in as-grown GaAs are found in the literature [34, 36]. In order to clarify the theoretical aspects, we have first calculated accurate formation energies for neutral Ga and As self-interstitials in GaAs. The results show that the minimum-energy configurations are the As$\langle 110 \rangle$ dumbbell and the Ga tetrahedral, with formation energies of 4.07 and 2.98 eV, respectively. The reliability of the calculations has been checked with respect to the spurious dispersion of the localized states and the elastic interactions between the periodic defect images. The obtained formation energies do not exclude the presence of Ga self-interstitials, whose formation energy is only 0.5 eV higher than for the As antisite in bulk GaAs. In contrast, the presence of As self-interstitials in as-grown GaAs is unlikely because their formation energy is 1.5 eV higher than that for the As antisite. There are indications that in as-grown LT GaAs the antisites must play the main role in explaining the lattice expansion and the ion-channelling data [34]. However, in the case of ion-implanted GaAs, we expect that As as well as Ga interstitials are both present in non-negligible concentrations and, due to their high mobility, can easily form complexes. We have concentrated our analysis on As self-interstitial clustering, because the insulating properties induced by ion implantation in GaAs, analogous to the insulating properties that characterize LT grown GaAs, seem to be related to As defects. In particular, the neutral As di-interstitial and the split antisite have been studied extensively. The results show in the former case remarkably large binding energies, implying that the As di-interstitial is most likely to form upon annealing. This complex is not detectable by DLTS, EPR or MCD and could explain why As self-interstitials are not detected even in as-implanted GaAs. The binding energy of the split antisite is 1 eV lower than that for the di-interstitial. On the basis of the split antisite properties and experimental results reported in the literature, we have discussed the possible presence of such a complex in GaAs (both LT grown and as implanted). The conclusion is that this complex is unlikely to be responsible for the donor band detected in LT grown GaAs.

Acknowledgments

This research has been supported by the Academy of Finland through their Centers of Excellence Programme (2000–2005). The authors wish to acknowledge the Center for Scientific Computing (CSC) for the generous computing resources.

References

[1] Bourgoin J C, von Bardeleben H J and Stievenard D 1988 *J. Appl. Phys.* **64** R65
[2] Lai S T and Nener B D 1994 *J. Appl. Phys.* **75** 2354
[3] Pons D and Bourgoin J C 1985 *J. Phys. C: Solid State Phys.* **18** 3839
[4] Yokota K, Kuchii H, Nakamura K, Sakaguchi M, Tekano H and Ando Y 2000 *J. Appl. Phys.* **88** 5017
[5] Marcinkevicius S, Jagadish C, Tan H H, Kaminska M, Korona K, Adomavicius R and Krotus A 2000 *Appl. Phys. Lett.* **76** 1306
[6] Jorio A, Carlona C, Parentau M, Aktik C and Rowell N L 1996 *J. Appl. Phys.* **80** 1364
[7] de Souza J P, Danilov I and Boudinov H 1997 *J. Appl. Phys.* **81** 650
[8] Fujioka H *et al* 1995 *J. Appl. Phys.* **78** 1470
[9] Jagadish C, Tan H H, Krotkus A, Marcinkevicius S, Korona K and Kaminska M 1996 *Appl. Phys. Lett.* **68** 2225
[10] Zhang S B and Northrup J E 1991 *Phys. Rev. Lett.* **67** 2339
[11] Brown R A and Williams J S 1997 *Phys. Rev.* B **55** 12852
[12] Vitali G, Zollo G, Pizzuto C, Rossi M, Manno D and Kalitzova M 1996 *Appl. Phys. Lett.* **26** 4072
[13] Sadana D K, Sands T and Washburn J 1984 *Appl. Phys. Lett.* **44** 632
[14] Sands T, Sadana D K, Gronsky R and Washburn J 1984 *Appl. Phys. Lett.* **44** 874
[15] Zollo G, Pizzuto C, Vitali G, Kalitzova M and Manno D 2000 *J. Appl. Phys.* **88** 1806
[16] Staab T E M, Haugk M, Frauenheim Th and Leipner H S 1999 *Phys. Rev. Lett.* **83** 5519
[17] Chadi D J 1992 *Phys. Rev.* B **46** 9400
[18] Knights A P, Ruffel S and Simpson P J 2000 *J. Appl. Phys.* **87** 663
[19] Liu X, Prasad A, Chen W M, Kurpiewski A, Stoschek A, Liliental-Weber Z and Weber E R 1994 *Appl. Phys. Lett.* **65** 3002
[20] Look D C, Walters D C, Mier M, Stutz C E and Brierely S K 1992 *Appl. Phys. Lett.* **60** 2900
Knights A P, Ruffel S and Simpson P J 2000 *J. Appl. Phys.* **87** 663
[21] Hohenberg P and Kohn W 1964 *Phys. Rev.* B **136** 864
[22] Kohn W and Sham L J 1965 *Phys. Rev.* A **140** 1133
[23] Perdew J P and Zunger A 1981 *Phys. Rev.* B **23** 5048
[24] Ceperley D M and Alder B J 1980 *Phys. Rev. Lett.* **45** 566
[25] Hamann D R 1989 *Phys. Rev.* B **40** 2980
[26] Monkhorst H J and Pack J D 1976 *Phys. Rev.* B **13** 5188
[27] Kleinman L and Bylander D M 1982 *Phys. Rev. Lett.* **48** 1425
[28] Puska M J, Pöykkö S, Pesola M and Nieminen R M 1998 *Phys. Rev.* B **58** 1318
[29] Northrup J E and Zhang S B 1993 *Phys. Rev.* B **47** 6791
[30] Makov G and Payne M C 1995 *Phys. Rev.* B **51** 4014
[31] Pöykkö S, Puska M J and Nieminen R M 1996 *Phys. Rev.* B **53** 3813
[32] Kim J, Kirchhoff F, Aulbur W G, Wilkins J W, Khan F S and Kresse G 1999 *Phys. Rev. Lett.* **83** 1990
[33] Landmann J I, Morgan C G, Schick J T, Papoulias P and Kumar A 1997 *Phys. Rev.* B **55** 15581
[34] Staab T E M, Nieminen R M, Gebauer J, Krause-Rehberg R, Luysberg M, Haugk M and Frauenheim Th 2001 *Phys. Rev. Lett.* **87** 45504
[35] Yu K M, Kaminska M and Liliental-Weber Z 1992 *J. Appl. Phys.* **72** 2850
[36] Bosker G, Stolwijk N A, Thgordson J V, Sodervall U and Andersson T G 1998 *Phys. Rev. Lett.* **81** 3443